Electronic Supplementary Information

AgPd-MnO_x supported on carbon nanospheres: An efficient catalyst for dehydrogenation of formic acid

Xiaoyu Zhang, Ningzhao Shang, Xin Zhou, Cheng Feng*, Shutao Gao, Qiuhua Wu, Zhi Wang, Chun Wang*

College of Science, Agricultural University of Hebei, Baoding 071001, China

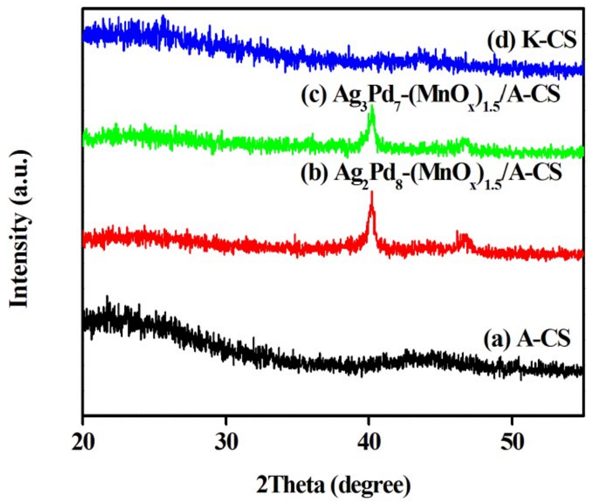

Fig. S1 X-ray diffraction patterns for as-prepared carbon spheres andAgPd-MnO_x/carbon spheres. (a) A-CS, (b) Ag_2Pd_8-$(MnO_x)_{1.5}$/A-CS, (c) Ag_3Pd_7-$(MnO_x)_{1.5}$/A-CS,(d) K-CS

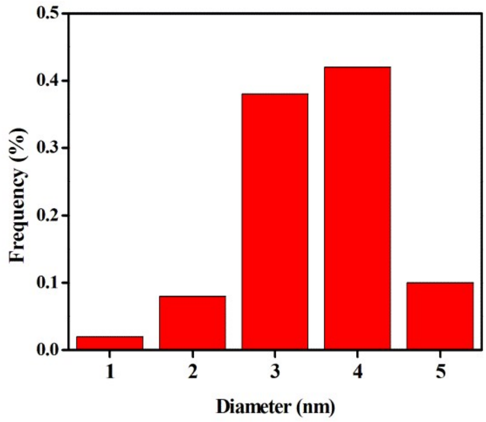

Fig. S2 The corresponding particle size distributions of Ag_1Pd_9-$(MnO_x)_{1.5}$/A-CS.

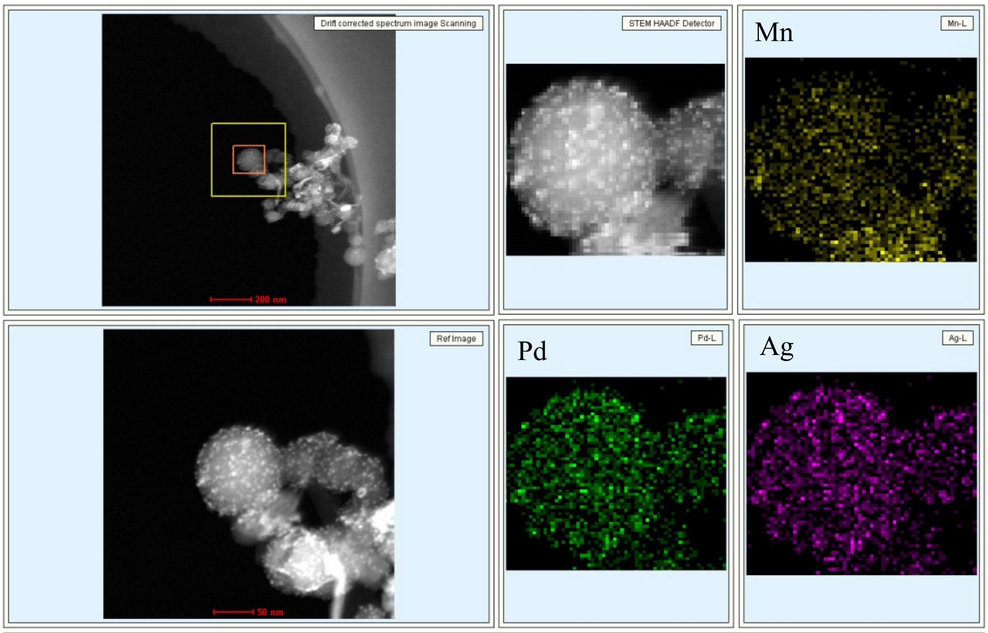

Fig. S3 The corresponding elemental mapping for Ag, Pd and Mn

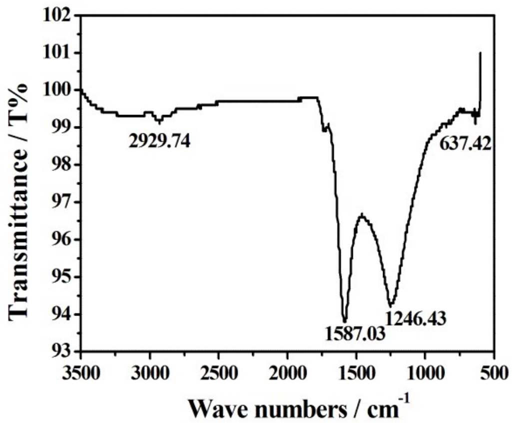

Fig. S4 The ATR FT-IR spectra of Ag_1Pd_9-$(MnO_x)_{1.5}$/A-CS

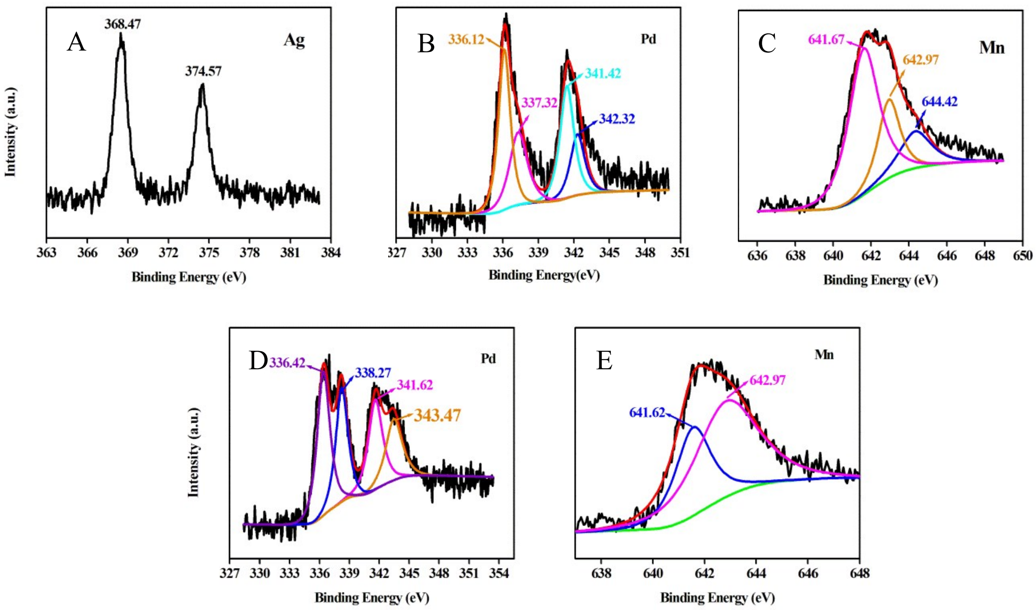

Fig. S5 XPS patterns of Ag_7Pd_3-$(MnO_x)_{1.5}$/A-CS (A, B and C) and Pd_{10}-$(MnO_x)_{1.5}$/A-CS (D and E)

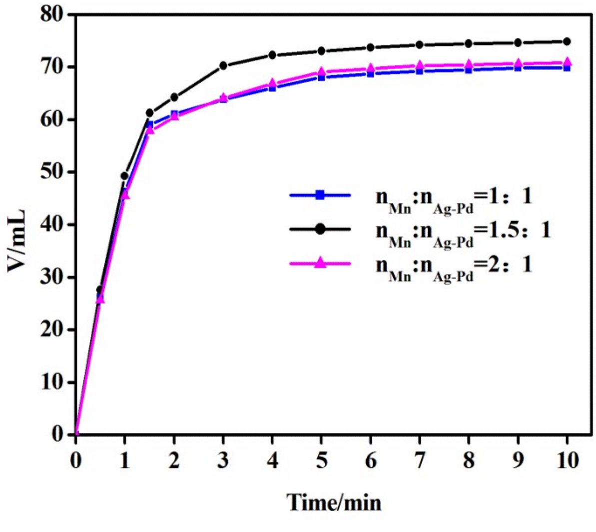

Fig. S6 Different molar ratios of Mn and Ag-Pd

(The reactions were performed at 50^{o}C, n_{FA}:n_{PF} = 2.5:7.5)

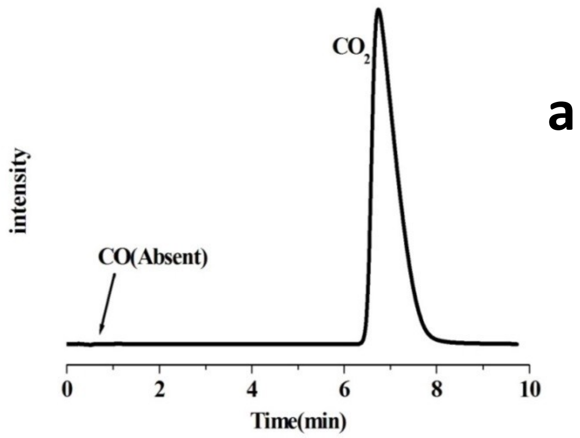

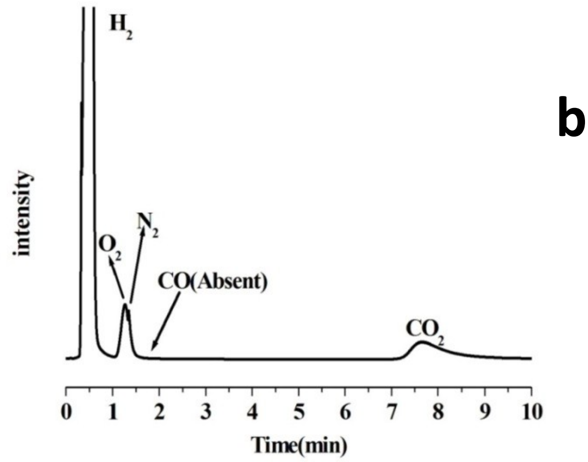

Fig. S7 GC spectrum using TCD for the evolved gas from FA/PF solution over Ag_1Pd_9-$(MnO_x)_{1.5}$/A-CS. The limit of detection for CO is 0.1 ppm.

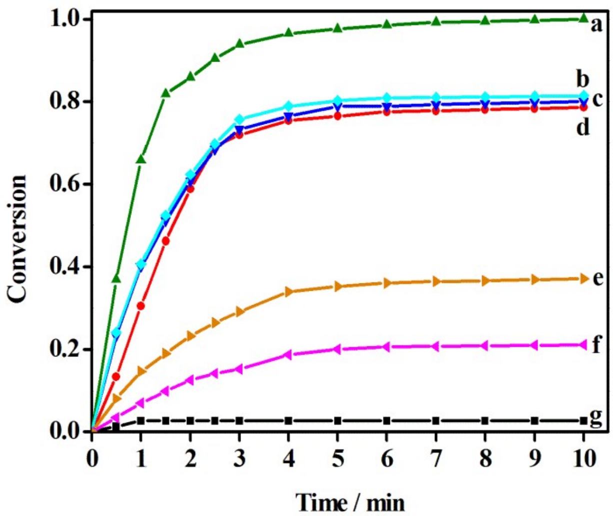

Fig. S8 Conversion of FA with different catalysts versus time at 50°C. (a)Ag_1Pd_9-$(MnO_x)_{1.5}$/A-CS, (b)Ag_3Pd_7-$(MnO_x)_{1.5}$/A-CS, (c)Ag_2Pd_8-$(MnO_x)_{1.5}$/A-CS, (d)Pd_{10}-$(MnO_x)_{1.5}$/A-CS, (e)Ag_7Pd_3-$(MnO_x)_{1.5}$/A-CS, (f)Ag_8Pd_2-$(MnO_x)_{1.5}$/A-CS), (g) Ag_{10}-$(MnO_x)_{1.5}$/A-CS)

(a)

(b)

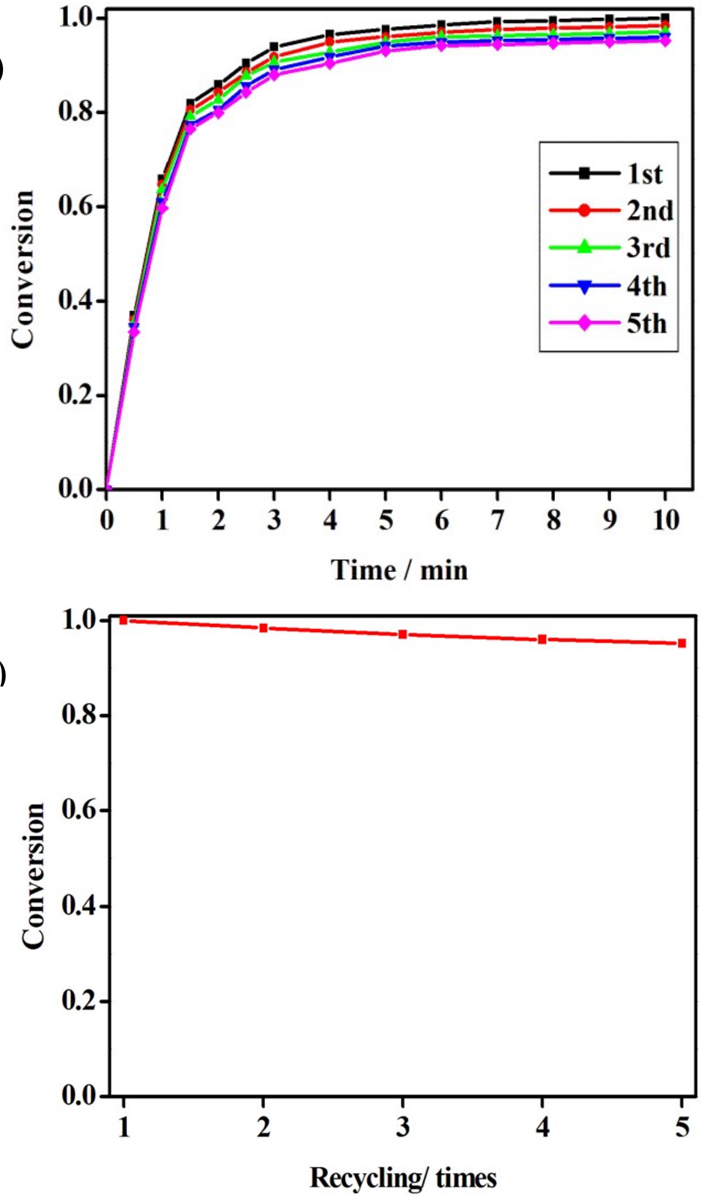

Fig. S9 Conversion of FA catalyzed by Ag_1Pd_9-$(MnO_x)_{1.5}$/A-CS versus time (a) and recycling times (b) at 50^{o}C.

Table S1 The dosages of reagents for the synthesis of different catalysts

Catalysts	CS/mg	$AgNO_3$/mL (1mg/mL)	H_2PdCl_4/mL (1mg/mL)	$MnSO_4$/mL (1mg/mL)
Ag_1Pd_9-$(MnO_x)_{1.5}$/A-CS	41	0.79	7.51	11.90
Ag_2Pd_8-$(MnO_x)_{1.5}$/A-CS	41	1.58	6.68	11.90
Ag_3Pd_7-$(MnO_x)_{1.5}$/A-CS	41	2.37	5.84	11.90
Ag_7Pd_3-$(MnO_x)_{1.5}$/A-CS	41	5.53	2.50	11.90
Ag_8Pd_2-$(MnO_x)_{1.5}$/A-CS	41	6.32	1.67	11.90
Ag_{10}-$(MnO_x)_{1.5}$/A-CS	41	7.9	0	11.90
Pd_{10}-$(MnO_x)_{1.5}$/A-CS	41	0	8.35	11.90
Ag_1Pd_9-$(MnO_x)_1$/A-CS	41	0.79	7.51	8.0
Ag_1Pd_9-$(MnO_x)_2$/A-CS	41	0.79	7.51	15.9

Table S2 The contents of Pd and Ag in AgPd-$(MnO_x)_{1.5}$/A-CS determined by ICP-AES

Catalysts	Ag (wt %)	Pd (wt %)	Initial mass ratio of Ag and Pd
Ag_1Pd_9-$(MnO_x)_{1.5}$/A-CS	0.97	8.92	1:9
Ag_2Pd_8-$(MnO_x)_{1.5}$/A-CS	1.96	7.94	2:8
Ag_3Pd_7-$(MnO_x)_{1.5}$/A-CS	2.92	6.90	3:7
Ag_7Pd_3-$(MnO_x)_{1.5}$/A-CS	6.91	2.91	7:3
Ag_8Pd_2-$(MnO_x)_{1.5}$/A-CS	7.93	1.95	8:2

Table S3 The N_2 adsorption-desorption isotherms of CS and Ag_1Pd_9-$(MnOx)_{1.5}$/CS

Sample	S_{BET} (m^2 g^{-1})	Pore volume (cm^3 g^{-1})	Pore diameter (nm)
A-CS	782.63	0.65	3.39
Ag_1Pd_9-$(MnO_x)_{1.5}$/A-CS	722.47	0.61	3.30
K-CS	2084.06	1.08	2.08
Ag_1Pd_9-$(MnO_x)_{1.5}$/K-CS	1519.24	0.80	2.12